Available online at www.sciencedirect.com

ScienceDirect

Procedia CIRP 101 (2021) 134–137

www.elsevier.com/locate/procedia

9th CIRP Conference on High Performance Cutting (HPC 2020)

Clamping Modeling in Automotive Flexible Workpieces Machining

Said Moussavi[a], Mikhaïl Guskov[a], Jérôme Duchemin[a], Philippe Lorong[a,*]

[a]*PIMM Laboratory, Arts et Metiers Institute of Technology, CNRS, Cnam, HESAM Universite, 151 boulevard de l'Hopital, 75013 Paris, France*

Abstract

Predictive dynamic simulations of virtual machining rely on accurate representation of eigenmodes and damping factors. Historically, the modeling of flexible workpieces requires experimental updating of general modal properties, especially due to a simplified definition of fixtures. In the present work a substructuring-based approach for a virtual machining simulation is developed. It is demonstrated on a vibration-prone boring of a thin-walled automotive workpiece. Fixture-affected zones are modeled via MacNeal-type approach. This enables for addressing the influence of clamping in the mechanical modeling of dynamics, and for creating specific models of typical fixture configuration. During simulation vibrations occur on similar frequencies to those observed on real machining. Resulting surface defects follow alike patterns in simulation and experiment.

Keywords: fixture modeling; flexible workpiece machining; dynamic modeling

1. Introduction

Vibratory risks constitute an important issue in machining flexible workpieces, which is often the case for highly valuable components. Various kinds of virtual machining solutions are increasingly used for designing machining processes [1], but as for vibrations, their outcomes are still rather qualitative, and to obtain realistic values, experiments are necessary.

As soon as one seeks, by a virtual machining approach, to study the impact of vibrations on the geometry quality of the machined surfaces it is necessary to build dynamic models sufficiently representative of their actual behaviour. These models relate to the tool, the part and their attachments. It is rather easy to work out models for the part and for the tool when they are free of attachment (they are generally in one piece and for tools inserts and their fixture do not have a significant impact) thanks to finite elements (FE) models with associated eigenmodes. The difficulties arise when it comes to modelling them assembled with the machine. For the tool, the attachment can have flexibilities and induce dissipation as well as the spindle whose dynamic behaviour, if it plays a role in the machining considered, is difficult to predict. For the part, flexibilities and dissipative effects are often localized around the contact with the fixture system. It is therefore interesting to have a strategy to model these assemblies.

In this work we are interested in cases where parts fixture is carried out thanks to a series of similar localized supports. This is common for cast parts, parts typically encountered in the automotive industry. We start by introducing a simple parameterized model for each of the connections between the part and the machining setup. The parameters are then optimized to minimize the difference between experimental data (transfer functions obtained by hammer impacts and accelerometers) and that produced by the FE model. This minimization requires the use of a reduced model to be achieved in reasonable time. Indeed, for complex parts, it is common to have FE meshes of several hundred nodes and it is not possible to do a FE analysis on a full model at each iteration during the optimization process. Such reduction can be performed via a MacNeal-type substructuring framework [2, 3]. Once the dynamical model is built the machining operation can be simulated in an integrated environment, including also models for tool-workpiece interaction and for machined surface evolution, via a framework similar to that of [4].

The machining operation case on which we develop our approach is briefly presented in section 2. Simplified models of localized fixtures are introduced section 3. Some details of the building of the reduced model are given section 4. In section 5 optimization results are shown. A discussion, illustrated by a machining simulation example, is provided section 6 before conclude in section 7.

* Corresponding author. Tel.: +33(0)1-4424-6285
E-mail address: philippe.lorong@ensam.eu (Philippe Lorong).

10.1016/j.procir.2021.04.004

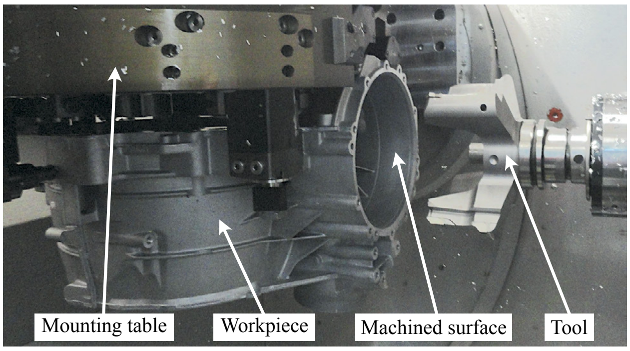

Fig. 1. Boring operation

2. Gearbox casing boring operation

We consider a boring operation carried out on an automotive part illustrated on Fig. 1. The workpiece, a gearbox casing, is a typical instance of a thin-walled part, fixed on the table by localized points (here: hydraulic clamps). The modeling of these fixtures are further discussed in section 3. The tool is a four tooth variable pitch PCD assembly.

An episode of chatter vibrations occurs during the boring of the bearing housing inner surface, involving dominant frequency contributions of 535 and 1205 Hz.

Both tool and workpiece (see Fig. 2) have numerous eigenfrequencies in the 2 kHz range . To assess the system's response during the operation, as well as for the modal analysis purposes, the workpiece was equipped with 7 accelerometers. These sensors were placed on the part so as to maximize the visibility of eigenmodes, according to the framework proposed by Balmes [5], with help of SDT software [6]. Similar procedure was applied for the tool characterization.

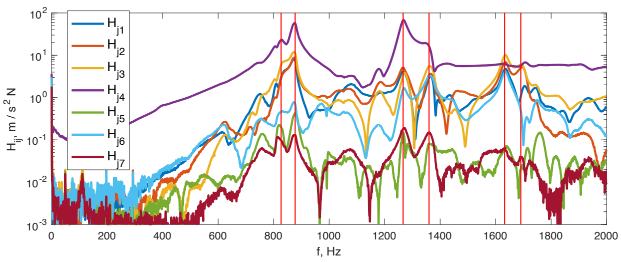

Fig. 2. Workpiece FRF (hammer test input, accelerometer output)

At the design stage, typical modeling approach for fixtures is perfect clamping. This would cause to approximate a prediction for eigenmodes before the industrial clamping system is prototyped.

3. Localized support modelling

When small surfaces of the part are in contact with the clamping system a simple way to take into account the small deformations occurring in this area is to consider these surfaces as rigid and to link them thanks to a master node (one for each contact surface) to no dimensional translational and rotational springs. In our case as there are 4 contact zones (Fig. 3), 4 master nodes have therefore been introduced. Each master node has 6 degrees of freedom : 3 translations and 3 rotations.

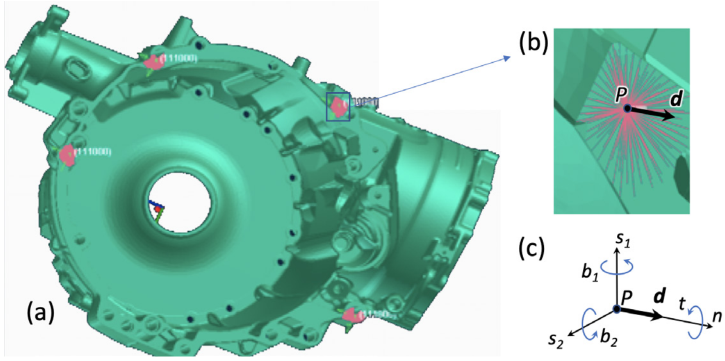

Fig. 3. Mounting configuration: (a) Location of 4 contacts; (b) kinematic links (pink) with master node (enlargement); (c) directions for stiffness parameters

In order to minimize the number of parameters we propose to simplify the model: stiffnesses in the normal direction are differentiated from those in the other two directions which are taken identical. Thus, only 4 stiffnesses are to be identified.

The sum up of the data defining a contact i are:

- the location of the master node P_i (geometric barycenter of the contact),
- the normal to the contact $\boldsymbol{d}_i$ (unit vector),
- in $\boldsymbol{d}_i$ direction, a translational (normal) stiffness and a rotational (torsion) stiffness: k_n and k_t,
- a shear stiffness and a bending stiffness in the two other directions: k_s and k_b.

4. Reduced FE model

To determine the 4 previously defined stiffness parameters, it is proposed to use a reduced model using a modal basis (30 eigenmodes in our example) enriched by static deformed shapes coming from unitary loading (unit forces or unit torques) applied on the master nodes (that means 6 shapes for each of the 4 contact areas). For the gearbox example the Residual Modes feature of the VPS (Virtual Performance Solution [7]) solver of the ESI company were used to compute eigen modes and static shapes of the final 54 Degrees of Freedom (DoF) system.

For this computation an initial estimation of the contact stiffnesses where used. In order to correct this initial estimation the approach consists in: i) directly modify the reduced 54 DoF system by adding stiffness corrections, ii) compute eigenmodes of the corrected reduced system, iii) compare these obtained result with experimental data (experimental eigenfrequency and shape of experimental eigenmode at the location of the sensors).

The way to obtain and modify the reduced system is as follows.

The load cases used to compute residual modes can be defined through column $\underline{S}_i$ such that:

$$\boldsymbol{U}(P_i) \cdot \boldsymbol{d}_i = \underline{S}_i^T \ \underline{q}, \tag{1}$$

where $\boldsymbol{U}(P_i)$ is the displacement (vector) at P_i and $\underline{q}$ the column containing all the degrees of freedom of the finite elements mesh. If P_i is located on a node of the mesh, $\underline{S}_i$ is a simple projection of degrees of freedom of this node on the unit vector $\boldsymbol{d}_i$. If it is not the case, the shape functions of the element containing P_i are needed. A simple approximation may be to use the nearest node to P_i.

The corresponding load case is then defined by a unit force or torque $\boldsymbol{F}_i = \boldsymbol{d}_i$ located at P_i. The corresponding generalized finite elements load is thus $\underline{Q}_i = \underline{S}_i$. The final Ritz basis $\underline{\underline{T}}$ containing eigen modes (Dynamic modes) and complementary Static modes is:

$$\underline{\underline{T}} = \left[{}^D\underline{\underline{\phi}}, {}^S\underline{\underline{\phi}}\right] = \left[{}^D\underline{\phi}^1, \ldots, {}^D\underline{\phi}^{nD}, {}^S\underline{\phi}^1, \ldots, {}^S\underline{\phi}^{nS}\right]. \tag{2}$$

The approximation of $\underline{q}$ is build with $\underline{\underline{T}}$ and a new column of (reduced) degrees of freedom $\underline{\alpha}$ such that: $\underline{q}(t) \approx \underline{\underline{T}}\,\underline{\alpha}(t)$. Only the computation of $\underline{\underline{T}}$ is expensive and depends of the size of the FE mesh. The computation of $\underline{\underline{T}}_i$ is not expensive as $\underline{S}_i$ contains only a very small number of non-nul values. We can then introduce the stain energy as:

$$S = \frac{1}{2}\underline{q}^T \left[\underline{\underline{K}} + \sum_{i=1}^{n} \underline{S}_i\, k_i\, \underline{S}_i^T\right] \underline{q} \approx \frac{1}{2}\underline{\alpha}^T \left[\underline{\underline{\tilde{K}}} + \sum_{i=1}^{n} k_i\, \underline{\underline{\Phi}}_i\right] \underline{\alpha} \tag{3}$$

where $\underline{\underline{\Phi}}_i = \underline{\underline{T}}^T\, \underline{S}_i\, \underline{S}_i^T\, \underline{\underline{T}}$ and $\underline{\underline{\tilde{K}}} = \underline{\underline{T}}^T\, \underline{\underline{K}}\, \underline{\underline{T}}$ are constant.

The final reduced mass matrix $\underline{\underline{\tilde{M}}} = \underline{\underline{T}}^T\, \underline{\underline{M}}\, \underline{\underline{T}}$ and reduced stiffness matrix $\underline{\underline{\widehat{K}}} = \underline{\underline{\tilde{K}}} + \sum_{i=1}^{n} k_i\, \underline{\underline{\Phi}}_i$ are those used to compute eigenmodes and eigen frequencies faced with experimental results. Both $\underline{\underline{\tilde{M}}}$ and $\underline{\underline{\tilde{K}}}$ matrices are provided by VPS [7]. For a given set (k_s, k_b, k_n, k_t) the cost of this resolution is below 0.1 s, to be compared to a cost of 30 s for the unreduced system.

5. Optimization results

The analysis of Frequency Response Functions given Fig. 2 allow us, through a parametric identification [8] and help of SDT [6], to extract experimental eigenfrequency, associated damping ratio, and shape of eigenmodes at the location of the 7 used sensors. In order to compare these data with numerical eigenmodes and eigenfrequencies we have firstly selected dominant eigenfrequencies (vertical red lines on Fig. 2): 825 Hz, 869 Hz, 1269 Hz, 1345Hz, 1626 Hz and 1693 Hz. The optimisation procedure is then conducted in order to minimize frequency difference between paired eigenmodes. For present example, an experimental and a numerical eigenmode are said to be paired if, during the optimization : their MAC (Modal Assurance Criterion [9]) is greater than 70% and simultaneously their frequency relative difference is less than 7%.

Even if this demanding MAC is relatively low, it makes it possible, in our case, and for the 6 dominant eigenmodes chosen, to differentiate these eigenmodes during the optimization.

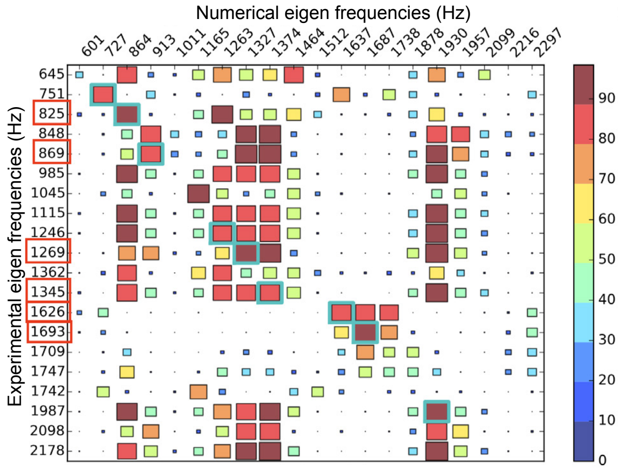

Fig. 4. MAC matrix for the part: experimental vs numerical. Dominant eigen frequencies are framed in red, Paired modes in light blue.

After optimization the obtained MAC matrix between experimental and numerical model is given Fig. 4 and relative error in Table 1. These results are obtained for the following values for contact stiffnesses: $k_n = 12.$ kN/μm, $k_s = 0.79$ kN/μm, $k_t = 700.$ kNm/μrad and $k_b = 1\,200.$ kNm/μrad.

Table 1. Part eigen frequencies: experimental vs numerical

Experimental frequency (Hz)	Numerical frequency (Hz)	Relative error
825.	864.	4.7%
869.	913	5.1 %
1269.	1327	4.6 %
1345.	1374.	2.2 %
1626.	1637.	0.7 %
1693.	1687.	-0.4 %

Same modeling and optimization strategy was used to take into acount the stiffness of the attachement of the tool. A mass has also been added (modification of the kinetic energy). The obtained MAC matrix for the tool, in its attachement, is given Fig. 5.

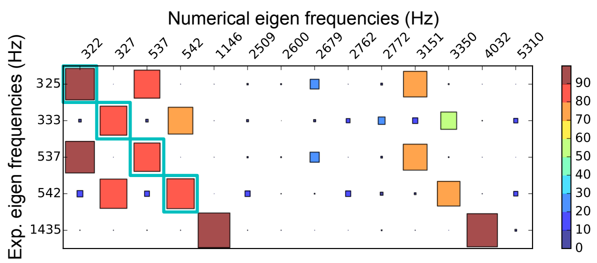

Fig. 5. MAC matrix for the tool: experimental vs numerical. Dominent eigen frequencies are framed in red, Paired modes in light blue.

The 2 first eigenmodes correspond to a first bending shape and the third and the fourth to a second bending shape. These results are obtained for the following values for contact stiffnesses: k_n = 50. kN/μm, k_s = 10. kN/μm, k_t = 2 500 kNm/μrad k_b = 500. kNm/μrad and m = 30.2 kg where the normal direction is (for the tool) its axial direction, the location of the master node at the geometric center of the attachment, and m an added mass at this location.

To complete the model, damping was introduced, via modal damping ratios obtained from modal testing.

6. Machining example and discussion

After obtaining the fixture stiffness parameters, the boring operation was simulated on the dynamical model thus updated, with dexel-based material removal model [4] and Kienzle type tool-workpiece interaction force model. The total duration of this time domain simulation is close to 30' on a standard computer (2.5 GHz, 4 Intel Core i7, 16 GB RAM).

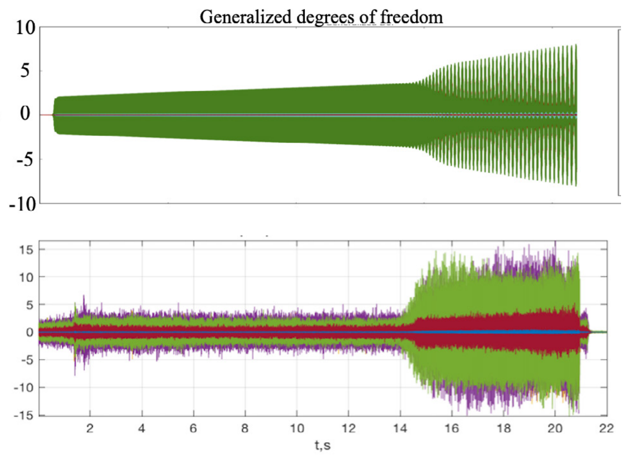

Fig. 6. Time record during machining. Top, Simulation: modal DOF response; bottom: Experiment, accelerometer signals

Response of the system recorded during machining, as presented on Fig. 6, manifest a remarkable change in level, occurring at similar timing. Resulting surface, shown on Fig. 7, feature chatter marks in similar areas. One can notice that, in the entry portion of the machined surface (apparently steady in the experiment), the simulation shows a minor defect pattern. This can be due, as suggested by [10], to the tool/matter interaction model not accounting for friction on the cylindrical machined surface.

7. Conclusion

The MacNeal-type substructuring approach, combined with a simplified contact zone model, offers an efficient tool for fixture parameters identification. This approach, applied to workpiece and tool enables realistic dynamical modeling in terms of vibratory characteristics relevant to machining. In the presented case of gearbox casing boring, a model was thus built in view of a time domain machining simulation. According to the results, the model features realistic chatter risks, as compared to the experimental observations.

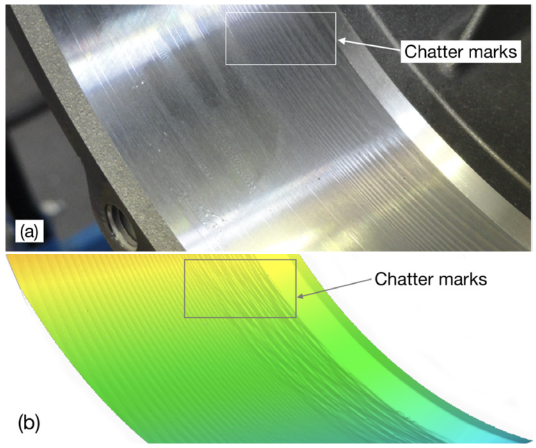

Fig. 7. Surface after machining: (a) Experiment; (b) Simulation

This type of model can be used both for stability studies and for temporal approaches. In a context of families of similar parts (similar shape and materials) whose attachments are also and very similar once a linkage model has been identified, it can be used for other parts and be used in other application cases to have the first predictive models without already having experimental data.

Acknowledgements

This work was done under grant of Bpifrance (the French Public Investment Bank) during IMPULSA FUI project. Industrial experiment were done on a machine tool inside the PCI-SCEMM company.

References

[1] Kadir, A.A., Xu, X., Hämmerle, E., 2011. "Virtual machine tools and virtual machining – A technological review". Robotics and Computer-Integrated Manufacturing, 27, pp. 494–508.
[2] Géradin, M., Rixen, D., 2015. "Mechanical Vibrations – Theory and Application to Structural Dynamics". Wiley, isbn 978-1-118-90020-8.
[3] MacNeal, R.H., 1971. "A hybrid method of component mode synthesis". Comp. and Struc., 1(4), pp. 581–601.
[4] Lorong, P., Coffignal, G., Balmes, E., Guskov, M., Texier, A., 2012. "Simulation of a Finishing Operation: Milling of a Turbine Blade and Influence of Damping". ESDA 2012, ASME 2012 11th Biennal Conference on Engineering Systems design and analysis, Nantes, France.
[5] Balmes, E., 2005. "Orthogonal maximum sequence sensor placements algorithms for modal tests, expansion and visibility". in Proceedings of the 23rd International Modal Analysis Conference (IMAC-XXIII '05), Orlando, Fla, USA.
[6] Structural Dynamic Toolbox, www.sdtools.com.
[7] Virtual Performance Solution, www.esi-group.com/software-solutions /virtual-performance/virtual-performance-solution.
[8] Richardson, M., Formenti, D., 1985. "Global curve fitting of frequency response measurements using the rational fraction polynomial method". International Modal Analysis Conference, pp. 390–397.
[9] Pastor, M., Binda, M., Harčarik, T., 2012. "Modal Assurance Criterion". Procedia Engineering, Vol. 48, pp. 543-548.
[10] Dilley, D., Bayly, P., Whitehead, B., Calvert, S., 2005, "An analytical study of the effect of process damping on reamer vibrations". Journal of Sound and Vibration, Vol. 280, pp. 997-1015.